# Efficiency-enhanced soliton optical parametric amplifier

**Silvia Carrasco Rodriguez, Juan P. Torres, and Lluis Torner**

*Laboratory of Photonics, Department of Signal Theory and Communications, Universitat Politecnica de Catalunya, Gran Capitan UPC-D3, Barcelona, ES 08034, Spain*

**Martin M. Fejer**

*E. L. Ginzton Laboratory, Stanford University, Stanford, California 94305*

Received July 23, 2001; revised manuscript received November 26, 2001

We show that the pump–to–signal power conversion efficiency of parametric chirped-pulse amplifiers made with periodically poled materials operating with multicolor spatial solitons can be significantly enhanced by employing engineered quasi-phase-matching gratings. Applications include compact sources of high-energy ultrashort pulses in diffraction-limited high-quality beams. © 2002 Optical Society of America

*OCIS codes:* 190.4410, 190.4420, 190.5530.

Important practical applications of high-energy femtosecond laser sources are emerging in a variety of fields, including material processing, biotechnology, medicine, environmental monitoring, and ultrafast chemistry. Thus the development of compact and reliable sources with energies in the microjoule–to–millijoule range is of current high technological interest. Since it is difficult at present to build laser oscillators generating such high-energy ultrafast pulses, laser amplifiers are generally used to increase the energy in low-power seed pulses. To avoid undesirable nonlinear effects in the amplifier, the peak power for a given pulse energy is reduced through the use of chirped-pulse amplification, with the ultrafast pulse stretched to a duration of the order of 1 ns.[1] Since the single-pass gain of typical laser amplifiers is too low for these purposes, regenerative amplification is widely used.[2]

Recently parametric chirped-pulse amplification has been explored as a simpler, single-pass alternative to a regenerative laser amplifier, with efficient nanosecond-pump–to–femtosecond-output-pulse energy conversion in periodically poled lithium niobate (PPLN),[3] and periodically poled potassium titanyl phosphate.[4] In addition to its simplicity, parametric amplification has important advantages, such as no intrinsic bandwidth limitation or power dissipation and straightforward design techniques to yield gain at any desired wavelength. However, high-gain single-pass amplifiers can strongly distort the wavefront of the amplified beam if there is significant transverse variation in gain. The trade-offs in obtaining efficient energy extraction from a Gaussian pump beam while maintaining high-output-beam quality are complex in a saturated parametric amplifier, so systematic techniques for designing such devices are important. A potentially interesting solution involves the generation of a multicolor spatial soliton.

It is now well established that soliton formation is possible in a variety of three-wave parametric mixing in quadratic nonlinear crystals.[5–7] Soliton formation in parametric amplification was observed experimentally by Stegeman and co-workers[8] and by Di Trapani *et al.*[9] in bulk potassium titanyl phosphate and lithium triborate, respectively. Soliton formation in bulk PPLN has also been reported.[10] Operation of the parametric amplifier in the soliton regime allows cleaning up the pump signals and can potentially yield robust output light distributions. Operation in such a regime was demonstrated recently by Galvanauskas and co-workers[11] in a system consisting of a diode-pumped $Q$-switched microchip laser emitting 750-ps pump pulses at 1064 nm, a Yb fiber amplifier, a standard femtosecond Er-doped fiber oscillator producing a few milliwatts of 300-fs seed pulses at 1556 nm, and a PPLN-based bulk optical parametric amplifier. The system yielded 50–60 $\mu$J in 1-ps amplified signal pulses from up to 300-kW peak-power pump light. Here we show that operating the parametric amplifier in the soliton regime and employing properly engineered quasi-phase-matching (QPM) gratings can lead to a significant enhancement of the overall pump–to–signal power conversion efficiency. We also show that with engineered gratings the robustness of the device against variations of the operating conditions is improved.

We study parametric amplification of pulses with durations on the nanosecond scale; thus we assume that a cw model for the light evolution is justified. Spatial soliton formation in an aperiodically poled bulk quadratic nonlinear medium under conditions for cw optical parametric amplification is thus governed by the evolution equations

$$i\frac{\partial A_1}{\partial z} + \frac{1}{2k_1}\nabla_\perp^2 A_1 + K_1 A_2^* A_3 = 0,$$

$$i\frac{\partial A_2}{\partial z} + \frac{1}{2k_2}\nabla_\perp^2 A_2 + K_2 A_1^* A_3 = 0,$$

0740-3224/2002/061396-05$15.00 

$$i\frac{\partial A_3}{\partial z} + \frac{1}{2k_3}\nabla_\perp^2 A_3 - \Delta k(z)A_3 + K_3 A_1 A_2 = 0, \quad (1)$$

where $A_i$ $(i = 1, 2, 3)$ are the slowly varying envelopes of the signal, idler, and pump beams, respectively, in MKSA units; $k_i$ are the corresponding wave numbers; and $K_i = 2\omega_i^2 d_{\text{eff}}/k_i c^2$. Here $\omega_i$, with $\omega_3 = \omega_1 + \omega_2$, are the angular frequencies of the waves, $c$ is the velocity of light in vacuum, and $d_{\text{eff}}$ is the effective nonlinear coefficient. The residual phase mismatch existing between the waves in the aperiodically poled material is given by

$$\Delta k(z) = 2\pi\left(\frac{1}{\Lambda_0} - \frac{1}{\Lambda(z)}\right), \quad (2)$$

where $\Lambda(z)$ is the local period of the aperiodically poled structure, and $\Lambda_0 = 2\pi/\Delta k_0$, with $\Delta k_0 = k_1 + k_2 - k_3$, is the period for exact phase matching.

To allow direct comparison with experimental data of existing and potential parametric amplifiers, all the calculations presented in this paper were performed with the actual parameters of PPLN pumped at 1064 nm. However, the results and trends reported are intended to be general. In particular, we set $d_{\text{eff}} \simeq 17$ pm/V, a waist of the pump beam of $w \sim 20\ \mu$m (FWHM $\sim$33 $\mu$m), and a device length $L = 35$ mm, but the results can be directly extended to parametric amplifiers built with different materials and operating wavelengths by use of the scaling properties of Eqs. (1). A transparent derivation of such scaling, with emphasis in the soliton regime, was discussed, e.g., by Menyuk and co-workers.[12]

The principle of operation of the efficiency-enhanced devices is based on the properties of the quadratic solitons as a function of the phase mismatch between the multiple waves that form the solitons.[13] In the parametric amplifier that is addressed here solitons form by the mutual trapping and locking of the pump, signal, and idler waves.[14] Solitons exist above a threshold light intensity at all values of the wave vector mismatch between the waves, but for a given total soliton power the corresponding sharing between the three waves that form the soliton depends on the actual value of the mismatch. Figure 1(a) shows the soliton power sharing for a fixed total power as a function of the normalized mismatch $\beta = k_1 w^2\, \Delta k$. The power imbalance between the signal and idler waves, defined as $P_{\text{im}} = P_1 - P_2$, is set to zero. The plot corresponds to a total power $P = 70$ kW. The share of the signal wave increases as $\beta$ becomes large and positive; thus only the region $\beta > 0$ is displayed. Figure 1(b) shows the threshold power for soliton existence as a function of $\beta$.

QPM techniques rely on the periodic modulation of the nonlinear properties of the medium to compensate for the existing wave vector mismatch between the waves.[15] In chirped QPM, the period is varied along the sample, hence yielding a longitudinally varying wave vector mismatch.[16,17] According to Fig. 1(a), the idea behind the scheme explored here is to employ chirped structures in which the mismatch between the waves goes from nearly zero at the input face of the crystal, where a large fraction of the soliton power is carried by the pump beam, to a large positive value at the end of the sample, where most of the soliton power is to be carried by the signal. The potential of the scheme arises from the ability of the solitons to adapt themselves to the local mismatch that they experience,[18,19] so that the overall pump-to-signal conversion efficiency might be optimized while the soliton nature of the beams is maintained. However, as is shown by Fig. 1(b), the larger the residual mismatch, the higher the threshold minimum power for soliton existence. Therefore, the question is whether the process actually enhances the efficiency and overall robustness of the soliton parametric amplifier as a function of the input pump power, the strength of the QPM chirp, and the largest achievable value of $\beta$ (i.e., the closest the ideal device performance is to the quantum limit).

To determine whether such is the case, we conducted comprehensive series of numerical experiments solving the system of Eqs. (1) for a variety of input light conditions and QPM chirps. We considered linear chirp profiles with the form

$$\frac{\mathrm{d}\beta(z)}{\mathrm{d}z} = \frac{\beta(L) - \beta(0)}{L}, \quad (3)$$

and we verified that analogous results are obtained with different profiles. In the numerical experiments shown here, we set the pump and the signal wavelengths at $\lambda_3 = 1.064\ \mu$m and $\lambda_1 = 1.556\ \mu$m, respectively; thus an

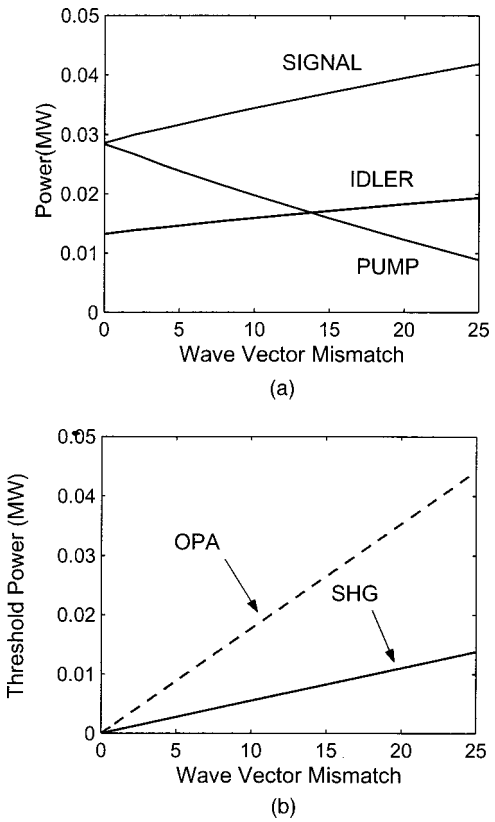


Fig. 1. (a) Power sharing between the pump, idler and, signal forming a soliton of total power 70 kW in PPLN, as a function of the normalized wave vector mismatch, for $\beta > 0$. (b) Power threshold for soliton existence. In the case of optical parametric amplification (OPA), $\lambda_1 = 1.556\ \mu$m, $\lambda_2 = 3.365\ \mu$m, $\lambda_3 = 1.064\ \mu$m. In the case of second-harmonic generation (SHG), $\lambda_1 = \lambda_2 = 1.556\ \mu$m, $\lambda_3 = 0.778\ \mu$m.

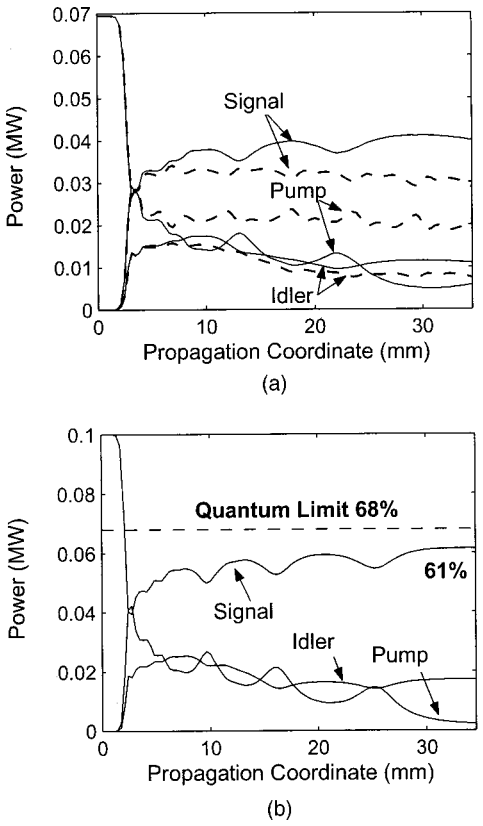


Fig. 2. Power carried by the pump, signal, and idler versus device length. (a) $P = 70$ kW; solid curves, chirped QPM sample with $\beta(0) = 0$, $\beta(L) = 15$; dashed curves, unchirped sample with $\beta(z) = 0$. (b) $P = 100$ kW, $\beta(0) = 0$, $\beta(L) = 25$. In all cases $L = 35$ mm.

idler wave is generated at $\lambda_2 = 3.365\,\mu$m. The input seed signal is assumed to carry a cw power of 30 mW in a Gaussian beam with a waist of 20 $\mu$m, but we verified that the results do not depend sensitively on these choices. Note that the maximum pump-to-signal energy conversion efficiency achievable is given by the quantum limit where all pump photons are downconverted into signal and idler photons, that is, by the ratio $\lambda_3/\lambda_1$. For the wavelengths given above, such a quantum limit amounts to a pump-to-signal energy conversion efficiency of $\approx$68%.

Figure 2(a) illustrates the difference between soliton parametric amplifiers employing periodic and aperiodic gratings. The plots show the evolution of the power carried by each wave along the device when the input pump carries 70 kW. The dashed curves correspond to a periodic structure featuring $\beta = 0$ all along the sample. A soliton is readily excited with a pump-to-signal power efficiency measured at the end of a device 35 mm long of $\approx$41% (i.e., $\approx$60% of the quantum limit). This means that $\approx$30% of the input power still remains at the pump wavelength. The solid curves show the light evolution under the same input conditions but now for the propagation in an aperiodic structure with a chirp that yields a value of the mismatch at the input and the output faces of the crystal of $\beta(0) = 0$, and $\beta(L) = 15$, respectively. The device efficiency increases up to 57% (i.e., $\approx$84% of the quantum limit), and the output beams feature the shape of the soliton associated with the corresponding local mismatch. As is suggested by Fig. 1(a), higher efficiencies can be obtained with stronger chirps that yield larger values of $\beta(L)$, even though higher input powers are also necessary to exceed the threshold for soliton existence. One finds that efficiencies in excess of 90% of the quantum limit are readily obtained in properly designed QPM chirps. Figure 2(b) shows a typical example when the input pump power amounts to 100 kW in a sample with $\beta(0) = 0$, $\beta(L) = 25$, which for the parameters of PPLN corresponds to a period variation of 1.1 $\mu$m over the sample length.

For the QPM-chirped soliton optical parametric amplifier to be of potential practical importance, the efficiency enhancement has to occur under a variety of conditions with improved performances relative to unchirped structures. Figure 3 suggests that this is indeed the case. In the plots displayed, the points are the results of the numerical experiments; the interpolated lines are only to help the eye. Figure 3(a), which shows the pump–to–signal power conversion efficiency as a function of the residual mismatch existing at the input face of the aperiodi-

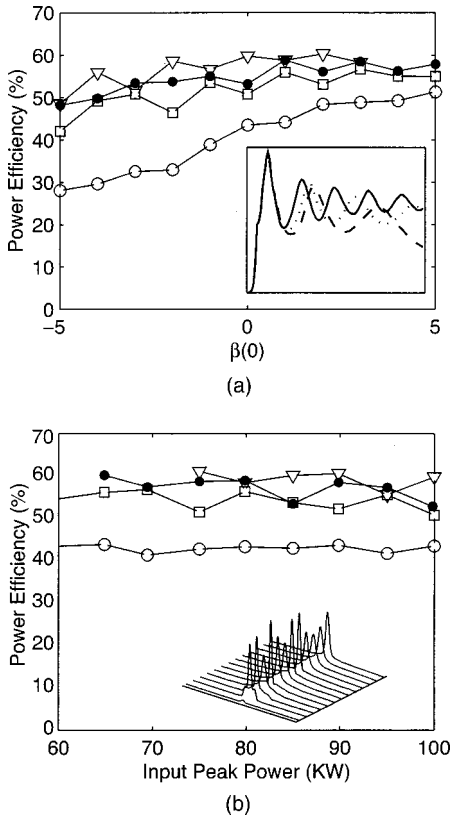


Fig. 3. (a) Pump-to-signal power conversion efficiency as a function of the normalized wave vector mismatch [$\beta(0)$] existing at the beginning of the QPM-chirped sample, for different QPM chirps. Open circles, unchirped sample with $\beta(z) = 0$; squares, $\beta(L) - \beta(0) = 10$; filled circles, $\beta(L) - \beta(0) = 15$; triangles, $\beta(L) - \beta(0) = 20$. In all cases $P = 100$ kW. Inset, peak amplitude of the signal beam as a function of the device length: $P = 100$ kW, $\beta(0) = 5$. Solid curve unchirped sample; dotted curve, $\beta(L) = 15$; dashed curve, $\beta(L) = 20$. (b) Efficiency as a function of input pump power with $\beta(0) = 0$, and different QPM chirps; symbols as above. Inset: Detail of the signal evolution; $P = 70$ kW, $\beta(L) = 15$.

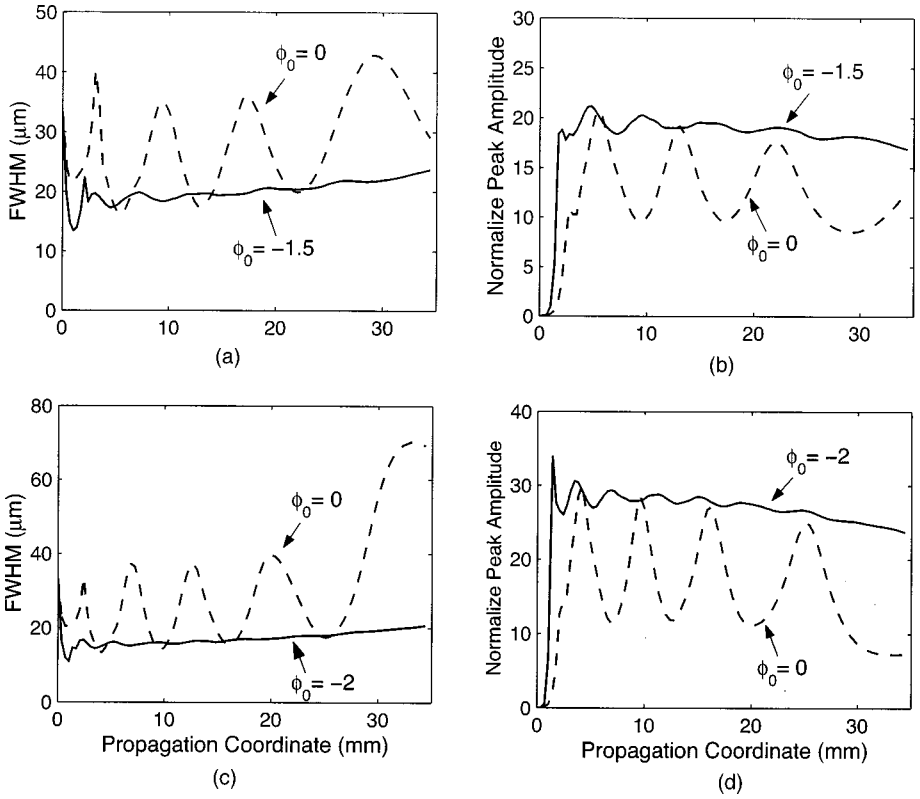


Fig. 4. Suppression of oscillations of the beam width and peak amplitude of the solitons by employing pump beams with curved wave fronts. The pump beam is $a_3(\xi = 0) = a_0 \exp[(-x/\eta)^2 + i\phi_0 x^2]$. Conditions: (a) and (b), $P = 70$ kW, $\beta(0) = 0$, $\beta(L) = 15$; (c) and (d), $P = 100$ kW, $\beta(0) = 0$, $\beta(L) = 25$.

cally poled crystal $\beta(0)$, reveals that the efficiency of the QPM-chirped soliton optical parametric amplifier exhibits a remarkable robustness against variations of the mismatch in the sample relative to the nominal value. Such deviations may appear, for example, because of slight deviations in the fabrication of the QPM domain length, or because of temperature oscillations in the oven that is supposed to hold the crystal at a constant temperature suitable for phase matching.

Figure 3(b) compares the pump-to-signal efficiency obtained for a range of input pump powers in different chirped and unchirped structures. For all pump powers shown, the efficiency is always higher in the chirped parametric amplifier than in an amplifier employing a structure with a constant residual mismatch. Also, the efficiency is found to be almost constant within a wide range of pump powers, indicating that a constant value should be obtained in a device pumped with pulsed light. Note that all cases shown in the plots correspond to the excitation of a multicolor soliton. It is worth mentioning that outside the corresponding ranges of mismatches $\beta(0)$ and pump powers, high energy-conversion efficiencies can also be obtained. However, when the input light and material conditions do not yield the excitation of a soliton, the output beam profiles might not feature the clean soliton shape.

The inset of Fig. 3(a) shows typical evolutions of the peak amplitudes of the signal beam as a function of the device length. The peak amplitudes, and hence the beam widths, undergo large oscillations. This is a potential drawback of the soliton optical parametric amplifier that

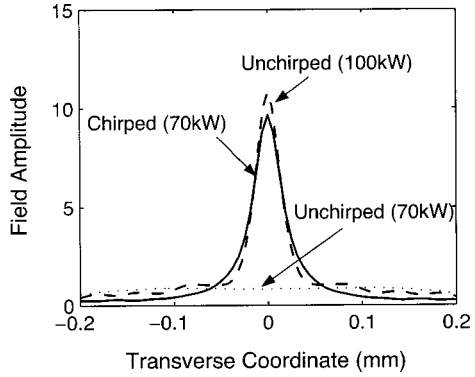


Fig. 5. Detail of the normalized amplitude of the output signal beam for different conditions. Solid curve $P = 70$ kW, $\beta(0) = 0$, $\beta(L) = 10$; dotted and dashed curves, unchirped sample with $\beta(z) = 10$, and $P = 70$ kW and $P = 100$ kW, respectively.

may be attributed to the internal modes of the multicolor solitons[20,21] that are typically present in their excitation with arbitrary input signals. Schemes that allow reduction of such oscillations need to be elaborated. A potential solution is to use pump beams with curved wave fronts, a typical example of which is shown in Fig. 4. The conclusion is that a drastic reduction of the oscillations of the peak amplitude and beam width of the excited solitons can be achieved.

The potential of the QPM-chirped structures suggested by Figs. 2 and 3 is further illustrated by Fig. 5. The plot shows that even though similar efficiencies and output beams might be obtained in chirped and in optimized unchirped structures [here $\beta(z) = 10$] when the input power

is high enough (here $P = 100$ kW), when $P$ is reduced (here to 70 kW) only with the device employing the chirped QPM is a high brightness soliton generated, while no soliton is formed in the unchirped sample. The drastic difference between the shapes of the output signals that are obtained in both cases is clearly visible.

To sum up, we have shown numerically that the overall performance of optical parametric chirped-pulse amplifiers made with periodically poled materials operating with multicolor spatial solitons can be significantly enhanced by employing engineered QPM gratings. Results analogous to those reported here were obtained for a variety of input pump and signal powers, shapes, and waists, QPM chirp strengths and profiles, and device lengths. To be specific, here we focused on aperiodically poled $LiNbO_3$, but results hold for all materials where QPM techniques can be implemented, including $KTiOPO_4$, $KNbO_3$, $LiTaO_3$, $RbTiOAsO_4$, and semiconductors.[22–25]

We conclude by noting that operation of the parametric amplifier in the soliton regime requires input light conditions employed in existing devices; thus the scheme presented here holds promise for experimental implementation.

## ACKNOWLEDGMENTS

This work was supported by the Generalitat de Catalunya, and by the Spanish Government under contract TIC2000-1010. M. M. Fejer acknowledges support by Air Force Office of Scientific Research/Air Force Materiel Command/U.S. Air Force. Numerics were carried out at the Centre Europeu de Paral.lelisme de Barcelona-IBM Research Institute.

S. C. Rodriguez may be reached by e-mail at carrasco @tsc.upc.es.

## REFERENCES

1. D. Strickland and G. Mourou, "Compression of amplified chirped optical pulses," Opt. Commun. **56**, 219–221 (1985).
2. See, e.g., C. G. Durfee III, S. Backus, M. M. Murnane, and H. C. Kapteyn, "Design and implementation of a TW-class high-average power laser system," IEEE J. Sel. Top. Quantum Electron. **4**, 395–406 (1998).
3. A. Galvanauskas, A. Hariharan, D. Harter, M. A. Arbore, and M. M. Fejer, "High-energy femtosecond pulse amplification in a quasi-phase-matched parametric amplifier," Opt. Lett. **23**, 210–212 (1998).
4. J. Hellstrom, G. Karlsson, V. Pasiskevicius, and F. Laurell, "Optical parametric amplification in periodically poled $KTiOPO_4$ seeded by an Er-Yb:glass microchip laser," Opt. Lett. **26**, 352–354 (2001).
5. G. I. Stegeman, D. J. Hagan, and L. Torner, "$\chi^{(2)}$ cascading phenomena and their applications to all-optical signal processing, laser mode-locking, pulse compression, and solitons," Opt. Quantum Electron. **28**, 1691–1740 (1996).
6. L. Torner and G. I. Stegeman, "Multicolor solitons," Opt. Photon. News, June 2001, pp.36–39.
7. W. E. Torruellas, Z. Wang, D. J. Hagan, E. W. VanStryland, G. I. Stegeman, L. Torner, and C. R. Menyuk, "Observation of two-dimensional spatial solitary waves in a quadratic medium," Phys. Rev. Lett. **74**, 5036–5039 (1995).
8. M. T. G. Canva, R. A. Fuerst, S. Baboiu, G. I. Stegeman, and G. Assanto, "Quadratic spatial soliton generation by seeded down conversion of a strong harmonic pump beam," Opt. Lett. **22**, 1683–1685 (1997).
9. P. Di Trapani, G. Valiulis, W. Chinaglia, and A. Andreoni, "Two-dimensional spatial solitary waves from traveling-wave parametric amplification of the quantum noise," Phys. Rev. Lett. **80**, 265–268 (1998).
10. B. Bourliaguet, V. Couderc, A. Barthelemy, G. W. Ross, P. G. R. Smith, D. C. Hanna, and C. De Angelis, "Observation of quadratic spatial solitons in periodically poled lithium niobate," Opt. Lett. **24**, 1410–1412 (1999).
11. A. Galvanauskas, A. Hariharan, F. Raksi, K. K. Wong, D. Harter, G. Imeshev, and M. M. Fejer, "Generation of diffraction-limited femtosecond beams using spatially-multimode nanosecond pump sources in parametric chirped pulse amplification systems," *Conference on Lasers and Electro-Optics (CLEO)*, Vol. 39 of OSA Trends in Optics and Photonics Series (Optical Society of America, Washington, D.C., 2000), pp. 394–395.
12. C. R. Menyuk, R. Schick, and L. Torner, "Solitary waves due to $\chi^{(2)}$:$\chi^{(2)}$ cascading," J. Opt. Soc. Am. B **11**, 2434–2443 (1994).
13. L. Torner, "Amplification of quadratic solitons," Opt. Commun. **154**, 59–64 (1998).
14. A. V. Buryak, Yu. S. Kivshar, and S. Trillo, "Parametric spatial solitary waves due to type II second-harmonic generation," J. Opt. Soc. Am. B **14**, 3110–3118 (1997).
15. M. M. Fejer, G. A. Magel, D. H. Jundt, and R. L. Byer, "Quasi-phase-matched second harmonic generation: tuning and tolerances," IEEE J. Quantum Electron. **28**, 2631–2654 (1992).
16. M. A. Arbore, A. Galvanauskas, D. Harter, M. H. Chou, and M. M. Fejer, "Engineerable compression of ultrashort pulses by use of second-harmonic generation in chirped-period-poled lithium niobate," Opt. Lett. **22**, 1341–1343 (1997).
17. G. Imeshev, M. A. Arbore, M. M. Fejer, A. Galvanauskas, M. Fermann, and D. Harter, "Ultrashort-pulse second-harmonic generation with longitudinally nonuniform quasi-phase-matching gratings: pulse compression and shaping," J. Opt. Soc. Am. B **17**, 304–318 (2000).
18. L. Torner, C. B. Clausen, and M. M. Fejer, "Adiabatic shaping of quadratic solitons," Opt. Lett. **23**, 903–905 (1998).
19. S. Carrasco, J. P. Torres, L. Torner, and R. Schiek, "Engineerable generation of quadratic solitons in synthetic phase matching," Opt. Lett. **25**, 1273–1275 (2000).
20. C. Etrich, U. Peschel, F. Lederer, B. A. Malomed, and Yu. S. Kivshar, "Origin of the persistent oscillations of solitary waves in nonlinear quadratic media," Phys. Rev. E **54**, 4321–4324 (1996).
21. D. Artigas, L. Torner, and N. N. Akhmediev, "Dynamics of quadratic soliton excitation," Opt. Commun. **162**, 347–356 (1999).
22. M. Oron, M. Katz, D. Eger, G. Rosenman, and A. Skliar, "Highly efficient blue light generation in flux grown $KTiOPO_4$ periodically poled by an electric field," Electron. Lett. **33**, 807–809 (1997).
23. T. J. Edwards, G. A. Turnbull, M. H. Dunn, M. Ebrahimzadeh, H. Karlsson, G. Arvidsson, and F. Laurell, "Continuous-wave singly-resonant optical parametric oscillator based on periodically poled $RbTiOAsO_4$" Opt. Lett. **23**, 837–839 (1998).
24. J. S. Aitchison, M. W. Street, N. D. Whitbread, D. C. Hutchings, J. H. Marsh, G. T. Kennedy, and W. Sibbett, "Modulation of the second-order nonlinear tensor components in multiple-quantum-well structures," IEEE J. Sel. Top. Quantum Electron. **4**, 695–700 (1998).
25. J.-P. Meyn, M. E. Klein, D. Woll, R. Wallenstein, and D. Rytz, "Periodically poled potassium niobate for second-harmonic generation at 463 nm," Opt. Lett. **24**, 1154–1156 (1999).